PROCEEDINGS OF SPIE

SPIEDigitalLibrary.org/conference-proceedings-of-spie

Linewidth broadening factor and optical feedback sensitivity of silicon based quantum dot lasers

F. Grillot, J. Duan, H. Huang, B. Dong, D. Jung, et al.

F. Grillot, J. Duan, H. Huang, B. Dong, D. Jung, Z. Zhang, J. Norman, J. E. Bowers, "Linewidth broadening factor and optical feedback sensitivity of silicon based quantum dot lasers," Proc. SPIE 10939, Novel In-Plane Semiconductor Lasers XVIII, 109390N (1 March 2019); doi: 10.1117/12.2511762

SPIE.

Event: SPIE OPTO, 2019, San Francisco, California, United States

Linewidth broadening factor and feedback sensitivity of silicon based quantum dot lasers

F. Grillot[a,b,]*, J. Duan[a], H. Huang[a], B. Dong[a], D. Jung[c], Z. Zhang[d], J. Norman[e], and J. E. Bowers[c,d,e]

[a]*LTCI, Télécom ParisTech, 46 Rue Barrault, 75013 Paris, France;*
[b]*Center for High Technology Materials, University of New-Mexico, Albuquerque, NM 87106, USA;*
[c]*Institute for Energy Efficiency, University of California Santa Barbara, CA 93106, USA;*
[d]*Department of Electrical and Computer Engineering, University of California Santa Barbara, Santa Barbara, CA 93106, USA;*
[e]*Materials Department, University of California Santa Barbara, Santa Barbara, CA 93106, USA.*

ABSTRACT

The integration of optical functions on a microelectronic chip brings many innovative perspectives, along with the possibility to enhance the performances of photonic integrated circuits (PIC). Owing to the delta-like density of states, quantum dot lasers (QD) directly grown on silicon are very promising for achieving low-cost transmitters with high thermal stability and large insensitivity to optical reflections. This paper investigates the dynamical and nonlinear properties of silicon based QD lasers through the prism of the linewidth broadening factor (i.e. the so-called α-factor) and the optical feedback dynamics. Results demonstrate that InAs/GaAs p-doped QD lasers epitaxially grown on silicon exhibit very low α-factors, which directly transform into an ultra-large resistance against optical feedback. As opposed to what is observed in heterogeneously integrated quantum well (QW) lasers, no chaotic state occurs owing to the high level of QD size uniformity resulting in a near zero α-factor. Considering these results, this study suggests that QD lasers made with direct epitaxial growth is a powerful solution for integration into silicon CMOS technology, which requires both high thermal stability and feedback resistant lasers.

INTRODUCTION

Silicon photonics provides novel functionality and high performance for applications in short reach optical interconnects, board-to-board and chip-to-chip integrated photonics, laser based radars, self-driving cars and many others [1,2]. Silicon (Si) has been known for years to be a very efficient semiconductor material for waveguiding light in particular owing to the strong index contrast with silica [3]. However, the indirect bandgap of Si makes light emission from Si inefficient, and other techniques such as wafer- or flip-chip bonding must be investigated if light emission is to be realized [4]. Lasers integrated onto silicon are prone to optical reflections hence necessitating the inclusion of an expensive optical isolator [5]. This particular feature results from the existence of possible sub-cavities between the silicon on the gain material hence creating internal optical feedback, which when combined with external reflections can become highly problematic for the laser stability. Although recent research demonstrated an optical isolator operating for TE mode with 25 dB of isolation and 6.5 dB of insertion loss, their integration with lasers adds extra process steps and cost and poses significant design and fabrication challenges [6]. Therefore, the development of highly feedback insensitive transmitters is of paramount importance for silicon photonics. Furthermore, direct growth is indispensable for moving towards a fully integrated on silicon, efficient light source at low-cost with a high scalability and high yield [7,8]. In this context, InAs/GaAs quantum dot (QD) lasers using semiconductor atoms as a gain medium are ideal because they enable smaller devices, amplification with large thermal stability and strong integration cost advantages [9]. In this work, we investigate the dynamic and nonlinear properties of InAs/GaAs p-doped QD lasers epitaxially grown on silicon material via the linewidth broadening factor (α-factor) and the optical feedback dynamics. In the context of integrated photonics, analyzing the α-factor is of particular importance for evaluating not only the reflection sensitivity but also the emission line of future single mode lasers directly grown on silicon [10,11]. As opposed to hybrid semiconductor lasers heterogeneously integrated on silicon, QD lasers directly grown on silicon are found insensitive to optical perturbations without exhibiting any chaotic operation even if 100% of light is back reflected onto the laser facet. These initial results

Novel In-Plane Semiconductor Lasers XVIII, edited by Alexey A. Belyanin, Peter M. Smowton, Proc. of SPIE Vol. 10939, 109390N · © 2019 SPIE
CCC code: 0277-786X/19/$18 · doi: 10.1117/12.2511762

demonstrate the advantages of QD lasers for integrating photonics into silicon CMOS technology and for manufacturing future on-chip reflection insensitive transmitters.

QD LASER STRUCTURE

Figure 1(a) displays an atomic force microscopy image of uncapped InAs QDs grown on a GaAs/Si template. The QD density is typically about 5×10^{10} cm^{-2}. As shown in Figure 1(b), the QD laser epi-structure consists of five QD layers directly grown on an on-axis (001) Si wafer in a Veeco Gen-II molecular beam epitaxy chamber and spaced by 37.5 nm thick GaAs barrier layers. As already reported elsewhere, the photoluminescence spectrum revealed a full-width at half-maximum (FWHM) of about 30 meV from the ground state (GS) peak, hence indicating a highly homogeneous InAs QD size throughout the five QD stack [12]. As QD lasers are known to suffer from thermal broadening of carriers, p-doping is also used to improve the thermal stability [13]. For p-modulation doped QD lasers, the first 10 nm GaAs layer was undoped, followed by a 10 nm p-GaAs layer at a target hole concentration of 5×10^{17} cm^{-3} using Be. The final 17.5 nm GaAs layer was undoped again to complete the p-MD GaAs barrier. In what follows, both p-doped and undoped QD lasers are compared. Both devices are spatially single mode, namely Fabry-Perot (FP) with a ridge waveguide width of 3.5 microns. The front facet has a power reflectivity of 60% whereas a high reflectivity of 99% is used on the rear. The undoped (p-doped, respectively) QD laser is 1.1 mm (1.35 mm, respectively) long.

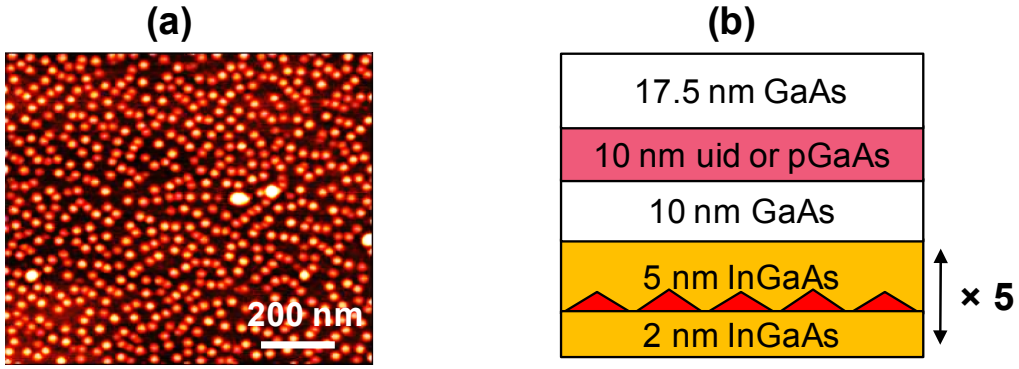

Figure 1. (a) Atomic force microscopy image of InAs QDs grown on a GaAs/Si template. The scale bar is 200 nm (b) The InAs/GaAs/Si QD laser epi-structure with gain media incorporating 5 QD stacks.

CONTINUOUS-WAVE OUTPUT CHARACTERISTICS

Figure 2 depicts the measured light current characteristics of the undoped (a) and p-doped (b) QD lasers for various temperatures ranging from 15ºC to 35ºC. The insets show the corresponding optical spectra measured at 3 times the threshold current. Both devices exhibit single state dynamics on the GS transition close to 1300 nm. The threshold current at room temperature (20ºC) for the undoped QD laser is 6 mA with an external efficiency of 17 %, while that of the p-doped laser is of 26.5 mA for an external efficiency of 6%. Overall, the excellent continuous-wave performance is attributed to the tight carrier confinement and from the strong reduction of dislocations and defects in the active region [14]. By varying the temperature from 15ºC to 35ºC, the threshold current increases from 5.3 mA to 8.3 mA for the undoped laser, whereas for the p-doped one, it increases from 26 mA to 28.5 mA. Although the p-modulated QD laser has a larger room temperature threshold current due to larger non-radiative recombination, its thermal stability is clearly improved, as depicted in Figure 2(b). Indeed, by introducing p-type modulation doping between dot layers, the thermal spreading of holes is reduced meaning that the temperature dependence of the gain is then set predominantly by the electron energy levels, which are widely spaced in energy.

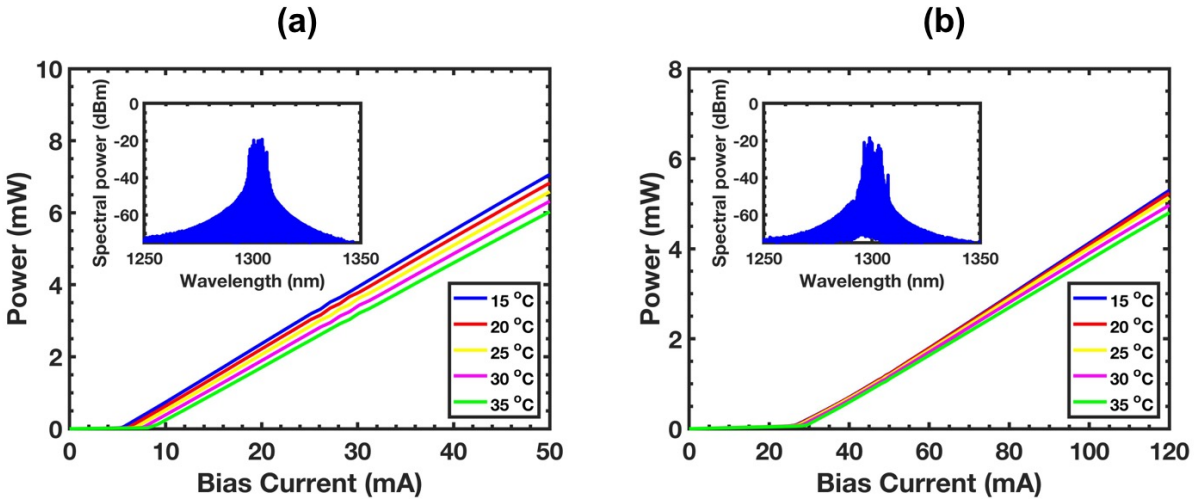

Figure 2. Light-current characteristics for the (a) undoped and (b) p-doped QD lasers. The temperature is varied from 15ºC to 35ºC. The insets show the corresponding optical spectra measured at 3 times the threshold current.

In a second part, the α-factor is extracted from the amplified spontaneous emission (ASE) which involves direct measurements of the differential gain and differential refractive index as a function of slight changes in the semiconductor laser carrier density operating in sub-threshold operation [15]. The differential index is measured by tracking the frequency shift of the longitudinal FP mode resonances, while the differential gain is obtained by measuring the net modal gain from the FP modulation depth in the ASE spectra. The differential gain is equivalent to the variation of net modal gain G, whose expression is given by the relationship:

$$G = \frac{1}{L}\ln\left(\frac{1}{\sqrt{R_1 R_2}}\frac{\sqrt{x}-1}{\sqrt{x}+1}\right) \quad (1)$$

with L the cavity length, x the ratio of the peak-to-valley intensity levels, R_1 and R_2 the front and back facet power reflectivities respectively. The α-factor is then retrieved as a function of measurable physical parameters through the well-established formula:

$$\alpha = -\frac{4n\pi}{\lambda_m^2}\frac{d\lambda_m/dI}{dG/dI} \quad (2)$$

with λ_m being the modal wavelength, n the optical index and I the sub-threshold bias current. The differential index is measured by tracking the frequency shift of the longitudinal FP mode resonances, while the differential gain is obtained by measuring the net modal gain from the FP modulation depth (gain ripple) in the ASE spectra. In the experiments, light from QD lasers is coupled into a 20 pm high-resolution optical spectrum analyzer via an antireflection coated lensed fiber. In order to properly extract the α-factor, any possible source of parasitic optical feedback must be fully eliminated from the setup by inserting an optical isolator after the laser. Last but not the least, in order to avoid any underestimation of the α-factor, it is fundamental to only account for the net carrier-induced frequency shift. As such, thermal effects are carefully eliminated by considering pulsed conditions with a pulse width of 100 ns whereas the device temperature is carefully monitored and kept constant throughout the measurements.

Figure 3 represents the net modal gain for undoped (a) and p-doped laser (b) for different subthreshold bias currents ranging from 0.9 times the threshold current to the threshold current. The net modal gain is found blue-shifted as the bias level increases reaching a value of about 3 cm^{-1} per QD layer at threshold for the undoped case against 2.4 cm^{-1} for the p-doped one. This difference simply results from the longer cavity length of the p-doped QD laser.

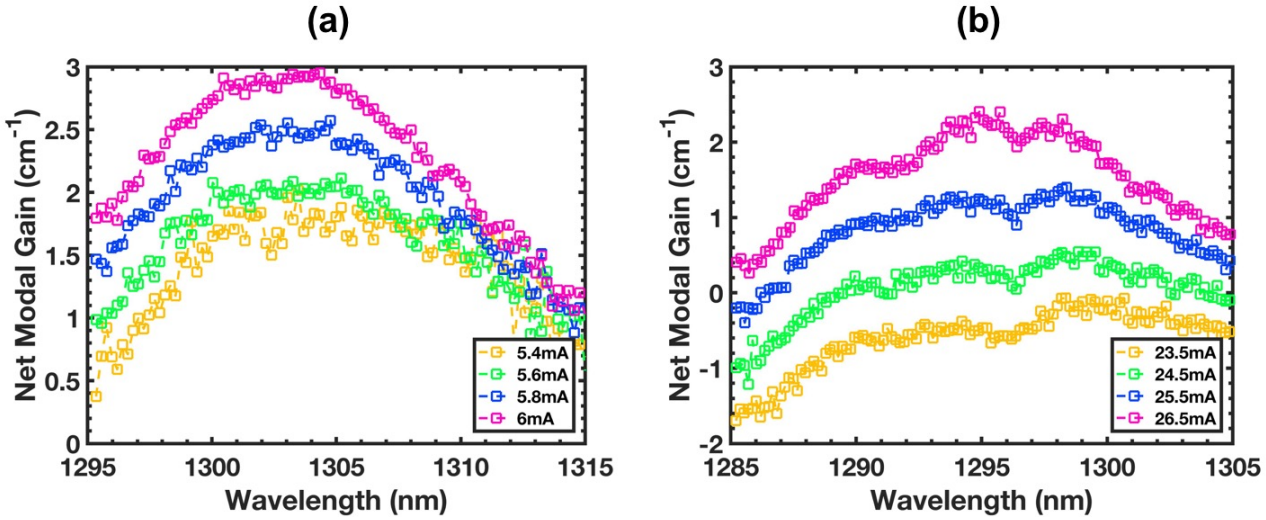

Figure 3. The net modal gain spectra for various subthreshold bias current conditions for the (a) undoped and (b) p-doped QD laser.

Figure 4 displays the spectral dependence of the α-factor measured at room temperature for the undoped and p-doped QD lasers. The dotted lines indicate the values at the gain peak. Here, we demonstrate ultra-low linewidth broadening factors for both lasers. Thus, the α-factor of the p-doped QD laser is found to be as low as 0.13 at the gain peak. This extremely low value directly results from the higher differential gain providing by the higher hole concentration. On the contrary, the undoped laser exhibits a slightly larger α-factor of 0.3 that is due to the increased transparency carrier density. Overall, we can conclude that these remarkable results are attributed to the very low threading dislocation density and the high dot uniformity in the laser active region.

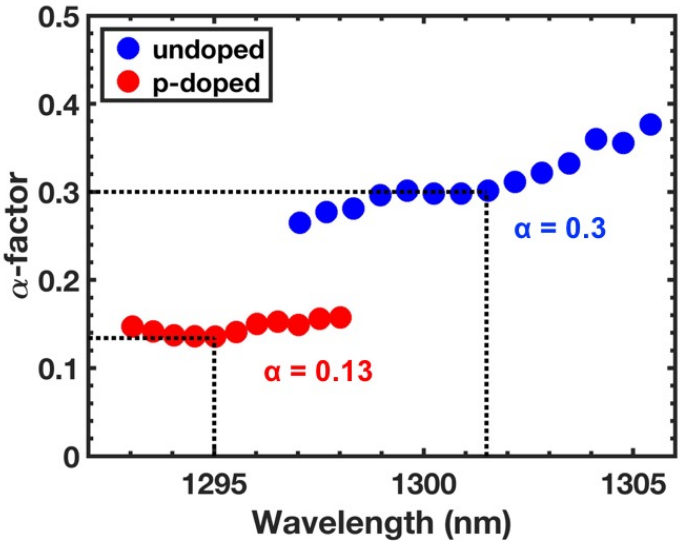

Figure 4. The measured α-factors for the undoped and p-doped QD lasers at room temperature (20ºC). The dotted line indicates the values taken at the gain peak.

Then, the temperature dependence of the α-factor is investigated for both p-doped and undoped QD lasers. Figure 5 presents the α-factor values corresponding to those taken at the gain peak for the temperature ranging from 15ºC to 35ºC with a step of 5ºC, the linear curve-fittings (dashed dotted lines) are used for guiding eyes only. As expected, the α-factor of the undoped laser slightly increases from 0.29 at 15ºC to 0.36 at 35ºC, while that of the p-doped device remains perfectly constant with a value of 0.13 over the same temperature range. For undoped QD lasers, the increase in the α-

factor with temperature is due to the increased occupancy in the non-resonant states which reduces the GS differential gain and increases the refractive index variations. On the other hand, for p-doped QD lasers, the refractive index variation is rather constant with temperature because the Auger recombination decreases, whereas those in the barrier and wetting layer increase.

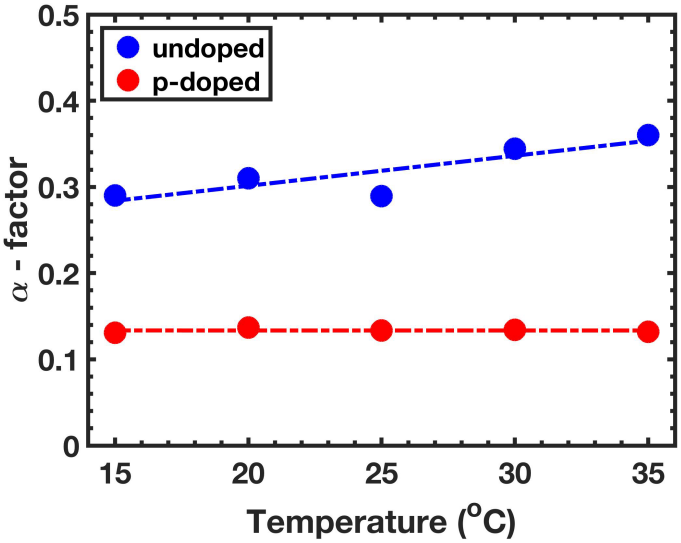

Figure 5. The α-factors as a function of temperature varying from 15ºC to 35ºC for p-doped (red) and undoped (blue) QD lasers. The linear curve-fittings (dashed dotted lines) are for guiding eyes only.

LASER RESPONSE TO OPTICAL FEEDBACK

In this section, the optical feedback sensitivity of the p-doped QD laser is analyzed. The QD laser is biased at three times the GS threshold current. The emission is coupled by an anti-reflection (AR) coated fiber, and 90% is sent to a backreflector (BKR), forming an external cavity with a 14 MHz fundamental frequency. The BKR is also used to continuously vary the feedback strength defined as the ratio between the returned power and the free-space emitted power at the coupling facet, from 0% to 18%. The maximal amount corresponds to 100% reflection from the external reflector onto the laser facet. The round trip coupling loss and splitter loss results in 18% reflection. The other 10% of the coupled power is isolated and amplified by a semiconductor optical amplifier (SOA). Then, another 90/10 is inserted to split 10% of the amplified power from the feedback laser for monitoring. An optical switch (SWT) is in place to swap the light between a power meter (PM), and optical or electrical spectrum analyzer (OSA or ESA). The rest of the 90% is externally-modulated by a Mach-Zehender modulator (MZM) at 10 GHz (on-off keying) with a pseudo-random binary sequence (PRBS) and a bit sequence length of 2^{31}-1. Afterwards, the modulated signal is pre-amplified and transmitted through a 2 km single-mode fiber (SMF). At the end, a variable optical attenuator (VOA) is used to tune the received power of the error detector in order to characterize the bit-error-rate (BER) performance. A high-speed oscilloscope (OSC) in used to capture the eye-diagram.

Figure 6(a) displays the longitudinal modes of the p-doped QD laser for the free-running case (i.e. without optical feedback) in red and for the highest feedback level (~18%) in blue. As shown, the feedback does not affect the modes e.g. no spectral broadening is observed, which is also confirmed by the mapping of the optical feedback dynamics performed in the electrical domain and displayed in Figure 6(b). Whatever the feedback strength, the laser does not show periodic or chaotic oscillations. In other words, the laser's reponse to the optical feedback exhibits a chaos-free operation i.e the so-called coherence collapse state is not observed in the experiments at least for the range of feedback under study. This effect is of course attributed to the very low α-factor and the large damping [8,12] but also to the fact that the laser emission remains on the GS transition. A recent work showed that ·a large ratio of the excited-to-ground-state lasing thresholds is beneficial for maintaining a high degree of stability in presence of optical feedback [16].. The p-

doped QD laser under study does not show any switching to the upper energy state whatever the bias current meaning that the excited-to-ground-state lasing threshold ratio is large. The same conclusion applies for the undoped QD laser with which no route to chaos is also observed up to six times the threshold current. Finally, Figures 6(c) and (d) show a comparison with a heterogeneously integrated QW laser on silicon. The device gets clearly disturbed at 1.7% optical feedback which corresponds to the first Hopf bifurcation beyond which the laser starts experiencing the route to chaos. Strong broadening of the FP modes as well as intense chaotic oscillations are observed.

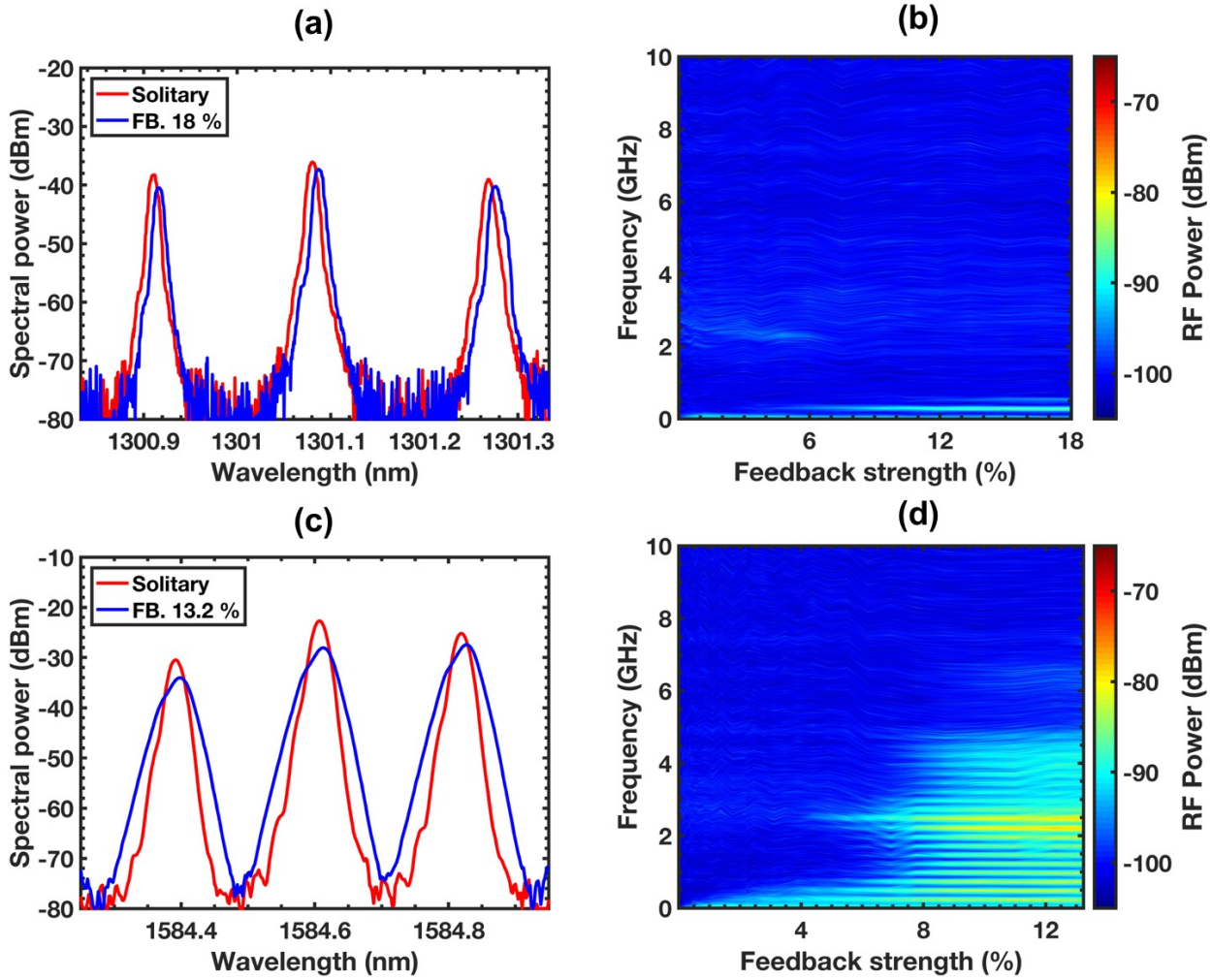

Figure 6. (a) Optical spectra and (b) RF spectral mappings of the p-doped QD laser on silicon as a function of the feedback strength at three times the threshold current; (c) Optical spectra and (d) RF spectral mappings of the heterogeneously integrated QW laser on silicon as a function of the feedback strength. The vertical axis is in logarithmic scale.

In what follows, testbed experiments are performed so as to highlight the effects of the feedback insensitivity from the end-user point of view. Figure 7 shows the bit error rate (BER) with and without optical feedback under 10 Gbps external modulation. As shown, whatever the configurations, BER plots between the free-running and the case for the highest feedback level (100% reflection on the laser facet) are perfectly overlapped hence implying an excellent stability of the QD laser without any performance degradation. Such a remarkable feedback resistance of the laser is once again attributed to the low α-factor associated to the absence of upper energy state emission for which it was shown that its switching at a very large bias prevents any optical feedback degradation [16]. Let us stress that the high damping is accentuated because of the epitaxial defects hence reducing the carrier lifetime through Shockley-Read-Hall recombination as recently demonstrated in a Ge-based QD laser which was shown to be more resistant to optical

feedback as compared to QD lasers made on a native GaAs substrate [17]. To sum, after transmission, a power penalty of 2.5 dB is obtained at 10^{-9} level, which is only due to the fiber chromatic dispersion and to the ASE induced noise. Despite that, the laser still achieves error-free operation for BER < 10^{-9}.

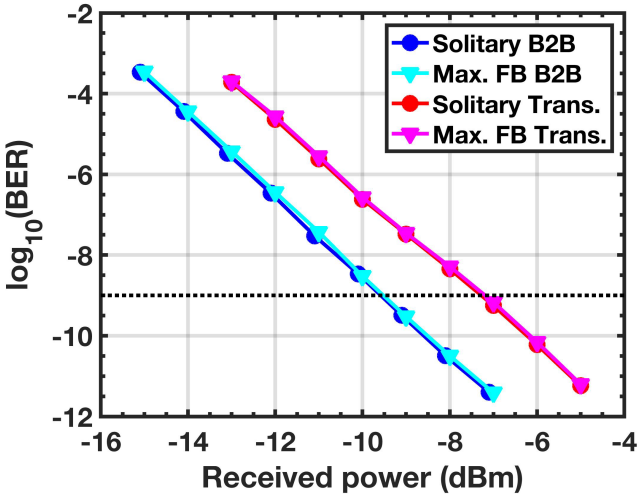

Figure 7. BER plots for: solitary QD laser in the back-to-back configuration (blue), QD laser with 100% optical feedback in the back-to-back configuration (cyan), solitary QD laser after transmission (red), QD laser with 100% optical feedback on the laser facet after transmission (magenta).

CONCLUSIONS

This paper focused on the dynamical and nonlinear properties of silicon based QD lasers directly grown on silicon. Results unveil very low α-factors, which directly transforms into a very large feedback insensitivity. No chaotic state occurs owing to the small α-factor, the low QD size inhomogeneity, the large damping rate, and the large excited-to-ground-state lasing threshold ratio. The latter is a figure of merit of the feedback dynamics hence a laser having a fast switching dynamics with respect to the bias current is more subject to destabilization by parasitic reflections. Finally, we proved that the reflection insensitivity also transforms into a 10 Gbps penalty-free operation with BER<10^{-9} between the free-running and the maximum optical feedback case. These results pave the way of future PICs operating without optical isolators. Future research will now consider feedback experiments in the short cavity regime as well as filtered optical feedback.

ACKNOWLEDGMENTS

Authors acknowledge the financial support of ARPA-E (DE-AR000067) and the Institut Mines-Télécom.

REFERENCES

[1] Norman, J. C., Jung, D., Wan, Y., and Bowers, J. E., "Perspective: The future of quantum dot photonic integrated circuits," APL Photonics, 3(3), 030901, (2018).
[2] Vivien, L. and Pavesi, L. Handbook of Silicon Photonics, (2014).
[3] Grillot, F., Vivien, L., Laval, S., Pascal, D., Cassan, E., "Size influence on the propagation loss induced by side-wall roughness in ultra-small SOI waveguides," IEEE Photon. Technol. Letts," 16(7), 1661(2004).
[4] Duan, G. H., Jany, C., Le Liepvre, A., Accard, A., Lamponi, M., Make, D., Kaspar, P., Levaufre, G., Girard, N., Lelarge, F., Fedeli, J. M., Descos, A., Ben Bakir, B., Messaoudene, S., Bordel, D., Menezo, S., de Valicourt, G., Keyvaninia, S., Roelkens, G., Van Thourhout, D., Thomson, D. J., Gardes, F. Y., and Reed, G. T., "Hybrid III-V on silicon lasers for photonic integrated circuits on silicon," IEEE J. of Selected Topics in Quantum Electron. 20, 6100213, (2014).

[5] Schires, K., Girard, N., Baili, G., Duan, G. H., Gomez, S., and Grillot, F., "Dynamics of Hybrid III-V Silicon Semiconductor Lasers for Integrated Photonics," IEEE Journal of Selected Topics in Quantum Electronics, 22(6), 43 (2016).
[6] Huang, D., Pinto, P., and Bowers, J. E., "Towards heterogeneous integration of optical isolators and circulators with lasers on silicon," Optical Materials Express, 8(9), 2471(2018).
[7] Kwoen, J., Jang, B., Lee, J., Kageyama, T., Watanabe, K., and Arakawa, Y., "All MBE grown InAs/GaAs quantum dot lasers on on-axis Si (001)," Optics Express, 26(9), 11568 (2018).
[8] Inoue, D., Jung, D., Norman, J., Wan, Y., Nishiyama, N., Arai, S., Gossard, A. C., and Bowers, J. E., "Directly modulated 1.3 μm quantum dot lasers epitaxially grown on silicon," Opt. Express 26(6), 7022(2018). □
[9] Eisenstein, G., and Bimberg, D., "Green Photonics and Electronics," Springer (2017).
[10] Duan, J., Huang, H., Lu, Z. G., Poole, P. J., Wang, C., and Grillot, F., "Narrow spectral linewidth in InAs/InP quantum dot distributed feedback lasers," Applied Physics Letters, 112(12), 121102, (2018).
[11] Becker, A., Sichkovskyi, V., Bjelica, M., Rippien, A., Schnabel, F., Kaiser, M., Eyal, O., Witzigmann, B., Eisenstein, G., and Reithmaier, J. P., "Widely tunable narrow-linewidth 1.5 μm light source based on a monolithically integrated quantum dot laser array," Applied Physics Letters, 110, 181103 (2017).
[12] Duan, J., Huang, H., Jung, D., Zhang, Z., Norman, J., Bowers, J. E., and Grillot, F., "Semiconductor quantum dot lasers epitaxially grown on silicon with low linewidth enhancement factor," Applied Physics Letters, 112(25), 251111, (2018).
[13] Crowley, M. T., Naderi, N. A., Su, H., Grillot, F., and Lester, L. F., "GaAs based quantum dot lasers," Advances in Semiconductor Lasers, 86(371), 42 (2012).
[14] Jung, D., Norman, J., Wan, Y., Liu, S., Herrick, R., Selvidge, J., Mukherjee, K., Gossard, A. C., and Bowers, J. E., "Recent Advances in InAs Quantum Dot Lasers Grown on On-Axis (001) Silicon by Molecular Beam Epitaxy," Phys. Status Solidi A, 1800602 (2018).
[15] Henning, I. D., and Collins, J. V., "Measurements of the semiconductor laser linewidth broadening factor," Electronics Letters, 19(22), 927(1983).
[16] Huang, H., Duan, J., Jung, D., Liu, A. Y., Zhang, Z, Norman, J., Bowers, J. E., and Grillot, F., "Analysis of the optical feedback dynamics in InAs/GaAs quantum dot lasers directly grown on silicon," Journal of the Optical Society of America B, 35(11), 2780(2018).
[17] Zhou, Y.-G, Zhao, X.-Y., Cao, C.-F., Gong, Q., and Wang, C., "High optical feedback tolerance of InAs/GaAs quantum dot lasers on germanium," Optics Express, 26(21), 28131(2018).